Journal of
**Applied Crystallography**
ISSN 0021-8898

Received 6 March 2000
Accepted 19 May 2000

# The disordered structure of tetraferrocenyl-[3]-cumulene, $(Fc)_2C{=}C{=}C{=}C(Fc)_2$, by simulated annealing using synchrotron powder diffraction data

**Robert E. Dinnebier,[a]* Manuela Schweiger,[b] Benno Bildstein,[b] Kenneth Shankland,[c] William I. F. David,[c] Andreas Jobst[a] and Sander van Smaalen[a]**

[a]Laboratory of Crystallography, University of Bayreuth, D-95440 Bayreuth, Germany, [b]Institut für Allgemeine, Anorganische und Theoretische Chemie, Universität Innsbruck, Innrain 52a, A-6020 Innsbruck, Austria, and [c]ISIS Facility, Rutherford Appleton Laboratory, Chilton, Didcot, Oxon OX11 0QX, England. Correspondence e-mail: robert.dinnebier@uni-bayreuth.de

In the molecular structure of tetraferrocenyl-[3]-cumulene, $(Fc)_2C{=}C{=}C{=}C(Fc)_2$, four ferrocene molecules are connected *via* a linear bridge consisting of four carbon atoms. At room temperature, the crystal structure has space group $P2_1/a$ ($Z = 1$) with $a = 13.104$ (5), $b = 6.121$ (2), $c = 11.194$ (4) Å, $\beta = 114.922$ (1)° and $V = 814.3$ (8) Å$^3$. A phase transition during cooling was not observed from room temperature to 75 K. From high-resolution X-ray powder diffraction data, the structure of the room-temperature phase was solved by the method of simulated annealing and refined by the Rietveld method using rigid bodies and restraints. The crystal structure was found to be highly disordered with the molecules occupying two orientations with equal probability and a 50% occupancy of the carbon atoms in the cumulene bridge. The disorder could be modelled by stacking faults in ordered structures. In contrast to other compounds of this class, the ferrocenyl groups are in a *syn* rather than in an up–down conformation with respect to the cumulene bridge.



## 1. Introduction

Bi- and polynuclear compounds with electroactive endgroups bridged by an unsaturated *sp* carbon chain are attracting much interest because of their unusual properties. From an application-oriented point of view, it is hoped to exploit these systems as materials for nonlinear optics, liquid crystals and molecular electronics. Metallacumulenes $[M]{=}(C{=}C)_n{=}[M]$ and metallaoligoalkynes $[M]{-}(C{\equiv}C)_n{-}[M]$ with various transition metal fragments $[M]$ are the most easily accessible compounds and therefore most widely investigated (Bruce, 1997, 1998; Paul & Lapinte, 1998; Touchard & Dixneuf, 1998).

In contrast to the above-cited work, our interest is focused on the synthesis and the study of the chemical and physical properties of organic cumulenes $R_2C_nR_2$ with organometallic endgroups ($R$ = ferrocenyl). So far we have prepared and characterized tetraferrocenylethylene, $(Fc)_2C{=}C(Fc)_2$ (Bildstein *et al.*, 1995), and the corresponding allene $(Fc)_2C{=}C{=}C(Fc)_2$ (Bildstein *et al.*, 1996), butatriene $(Fc)_2C{=}C{=}C{=}C(Fc)_2$ (Bildstein, Schweiger, Kopacka & Wurst, 1998), pentatetraene $(Fc)_2C{=}C{=}C{=}C{=}C(Fc)_2$ (Bildstein, Schweiger, Kopacka, Ongania & Wurst, 1998) and hexapentaene $(Fc)_2C{=}C{=}C{=}C{=}C{=}C(Fc)_2$ (Bildstein *et al.*, 1999). The ferrocenyl substituents in these cumulenes serve as redox-active moieties, electron donors and sterically protecting groups, thereby altering the reactivity and stability of these cumulenes in comparison to purely organic (Fischer, 1964; Hopf, 1980) non-ferrocenylated cumulenes. Standard X-ray single-crystal structure analyses have been possible for tetraferrocenylethylene (Bildstein *et al.*, 1995), -allene (Bildstein *et al.*, 1996) and -pentatetraene (Bildstein, Schweiger, Kopacka, Ongania & Wurst, 1998). In the case of tetraferrocenylethylene, severe steric congestion by the four ferrocenyl termini resulted in a non-planar and therefore chiral olefinic system (Bildstein *et al.*, 1995). Tetraferrocenylallene (Bildstein *et al.*, 1996) and tetraferrocenypentatetraene (Bildstein, Schweiger, Kopacka, Ongania & Wurst, 1998) showed regular molecular structures with orthogonal pairs of ferrocenyl substituents, as expected for cumulenes with an odd number of carbon atoms in the cumulene chain. All our attempts to obtain 'X-ray quality' single crystals of tetraferrocenylbutatriene (Bildstein, Schweiger, Kopacka & Wurst, 1998) and tetraferrocenylhexapentaene (Bildstein *et al.*, 1999) have failed. These cumulenes, with an even number of carbon atoms, are expected to have their two pairs of substituents in one plane and the ferrocenyl cylinders are anticipated to be arranged in an up–down manner, as has been observed in the other structures of ferrocenylcumulenes (Bildstein *et al.*, 1995, 1996; Bildstein, Schweiger, Kopacka, Ongania & Wurst, 1998).

In this contribution, we report on the crystal structure of tetraferrocenylbutatriene (tetraferrocenyl-[3]-cumulene) (Fig. 1) as determined from synchrotron radiation X-ray powder diffraction data using the methods of simulated annealing and Rietveld refinement. Tetraferrocenyl-[3]-cumulene is very stable, non-reactive and has poor solubility.

The complexity and accuracy of crystal structure refinements from powder data have been growing steadily since the pioneering work of Hugo Rietveld about 30 years ago (Rietveld, 1969). Nowadays, even the crystal structures of small proteins can be refined from high-resolution powder data (Von Dreele, 1999). On the other hand, it took another 20 years before a considerable number of structure determinations from powder diffraction data appeared in the literature (Le Bail, 1999). Most of these early 'powder structures' were solved by applying traditional methods for structure solution derived from methods for single-crystal data. With the development of real-space methods about 10 years ago, it became possible to determine the crystal structure of molecular compounds. As a prerequisite for the successful application of real-space methods, the connectivity within a group of atoms must be known prior to structure determination, which is often the case for molecules.

Grid search methods, of varying degrees of sophistication (*e.g.* Chernyshev & Schenk, 1998; Masciocchi *et al.*, 1993; Bendele *et al.*, 1998; Dinnebier *et al.*, 1995), were among the first direct-space algorithms. Monte Carlo (MC) techniques based on a random selection of structure configurations significantly outperform such grid searches and have allowed structures with around seven degrees of freedom to be determined (*e.g.* Tremayne *et al.*, 1996, 1997). Hence they were used mainly for rigid molecules with a few internal degrees of freedom. Simulated annealing is a logical extension of these simple MC approaches (Newsam *et al.*, 1992), allowing the crystal structure determination of fairly complex molecular compounds with several internal degrees of freedom (torsion angles) and several molecules in the asymmetric unit (*e.g.* Andreev & Bruce, 1998; Andreev, Lightfoot & Bruce, 1997; Andreev, MacGlashan & Bruce, 1997; David *et al.*, 1998; MacGlashan *et al.*, 1999). Recent advances in this field lie in an improved treatment of overlapping reflections, the development of faster algorithms and better annealing schedules (*e.g.* David *et al.*, 1998; Rius *et al.*, 1999).

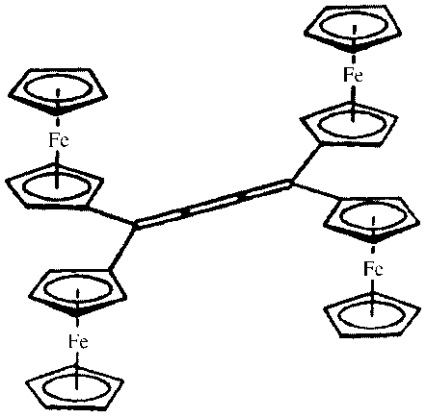


**Figure 1**
Schematic representation of the molecular structure of tetraferrocenyl-[3]-cumulene.

Among the various alternative approaches for structure determination from powder data are genetic algorithms to drive the parameter search (Kariuki *et al.*, 1999; Shankland *et al.*, 1997) and the minimization of the lattice energy (*e.g.* Schmidt & Dinnebier, 1999). The latter depends strongly on the quality of the potential parameters and the available computing power.

Lack of complete order makes the determination of the crystal structure more difficult. In the crystalline state, disorder may persist, which often leads to a higher symmetry of the structure than would have been possible without disorder. For many types of disorder, it is difficult to derive an appropriate model based on fixed atoms with harmonic atomic displacement parameters. It may be necessary to use many different sites, each one with a partial occupation of the atoms (*e.g.* Dinnebier *et al.*, 1999). Many additional parameters are introduced beyond those necessary for an ordered structure model, and high correlations between these parameters are often observed. Except for simple cases, these features make it quite complicated to refine disordered structures against powder diffraction data, because of the considerable reduction of information compared to single-crystal diffraction. In particular, the intensities are not known for many of the reflections. Therefore, Fourier maps, generated from the phases of the structure factors calculated for the 'best' model and their observed intensities, reveal information about the disorder in very special cases only.

In the present study, the simulated-annealing technique and consecutive Rietveld analysis were used for the determination of the disordered structure of tetraferrocenyl-[3]-cumulene. The tetraferrocenyl-[3]-cumulene molecule is present in two conformations, but the unit cell of the disordered structure is only half as large as the unit cell of any conceivable ordered structure of this compound.

## 2. Experimental

The synthesis of tetraferrocenyl-[3]-cumulene has been described elsewhere (Bildstein, Schweiger, Kopacka & Wurst, 1998).

Laboratory X-ray powder diffraction studies were performed at room temperature with a Nonius PDS120 diffractometer in transmission mode, equipped with a Ge(111) primary monochromator and a 120° 2Θ position-sensitive detector, using Cu $K\alpha_1$ radiation ($\lambda$ = 1.540598 Å) at 40 kV and 30 mA. The sample was sealed in a 0.3 mm glass capillary (Hilgenberg glass No. 50) and spun during measurement. Because of the low scattering power of the sample, the peak to background ratio was rather poor (Fig. 2). The sample was therefore measured for two days in order to accumulate enough intensity. Indexing of the X-ray powder diffraction pattern did not lead to the correct unit cell.

For the high-resolution X-ray powder diffraction experiments, the sample was sealed in glass capillaries of 0.5 mm

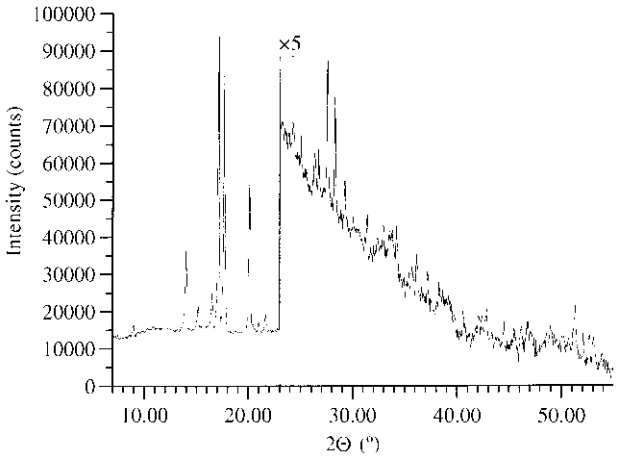


**Figure 2**
Scattered X-ray intensity for tetraferrocenyl-[3]-cumulene from a laboratory PDS120 diffractometer at ambient conditions as a function of diffraction angle 2Θ. The high-angle part is enlarged by a factor of 5 starting at 23° 2Θ. Wavelength λ = 1.54059 Å.

diameter (Hilgenberg glass No. 50). Powder diffraction data were collected at room temperature at beamline X3B1 at the National Synchrotron Light Source, Brookhaven National Laboratory (Table 1). X-rays of wavelength 0.70017 (2) Å were selected by a double Si(111) monochromator. The wavelength was calibrated with the NBS1976 alumina standard. The diffracted beam was analysed with a Ge(111) crystal and detected with a Na(Tl)I scintillation counter with a pulse-height discriminator in the counting chain. The intensity of the primary beam was monitored by an ion chamber. In this

**Table 1**
Crystallographic data for tetraferrocenyl-[3]-cumulene.

| | |
|---|---|
| Formula | $C_{44}H_{36}Fe_4$ |
| Temperature (K) | 295 |
| $M_r$ | 788.172 |
| Space group | $P2_1/a$ |
| $a$ (Å) | 13.104 (5) |
| $b$ (Å) | 6.121 (2) |
| $c$ (Å) | 11.194 (4) |
| $\beta$ (°) | 114.922 (1) |
| $V$ (Å$^3$) | 814.3 (8) |
| $Z$ | 1 |
| $D_x$ (g cm$^{-3}$) | 1.607 |
| $\mu$ (cm$^{-1}$) assuming calculated density | 16.79 |
| 2Θ range (°) | 2.0–40.4 |
| Step size (° 2Θ) | 0.005 |
| Counting time/step (s) | 10.6 (2.0–26.31° 2Θ); 6.3 (26.315–40.4° 2Θ) |
| Wavelength (Å) | 0.70017 (2) |

parallel-beam geometry, the resolution is determined by the analyser crystal instead of by slits (Cox, 1991). X-ray scattering intensities were recorded in steps of 0.005° for 10.6 s at each 2Θ from 2.0 to 26.31° and for 6.3 s at each 2Θ from 26.315 to 40.4° 2Θ (Fig. 3). The sample was spun around Θ during measurement to reduce grain-size effects. The powder pattern is characterized by a rapid fall off of intensity beyond $\sin\Theta/\lambda \simeq 0.13$ Å$^{-1}$. Peaks at low angle had a minimum full width at half-maximum of 0.008° 2Θ, which is close to the resolution of the spectrometer. Despite the rather long counting times, the maximum intensity in the strongest peaks is rather low with a maximum peak to background ratio of only 15:1.

Data reduction was performed using the program *GUFI*5.0 (Dinnebier & Finger, 1998). Indexing of the powder pattern using the program *ITO* (Visser, 1969) led to a primitive monoclinic unit cell with lattice parameters as given in Table 1. The space group could be determined unambiguously as $P2_1/a$ from the observed extinction rules. The number of formula units per unit cell, $Z = 1$, followed from packing considerations. No evidence for a superstructure was found.

From different batches of the title compound, several crystals which seemed to be suitable for single-crystal X-ray diffraction were picked and mounted at room temperature on a Mach3 diffractometer with a scintillation counter from Nonius BV, operated on a rotating anode with Mo $K\alpha$ radiation. A peak search over 12 h revealed only extremely weak and broad reflections, from which the cell parameters as determined from powder diffraction data could be confirmed. Owing to the mosaic spread of the sample, no reliable data for

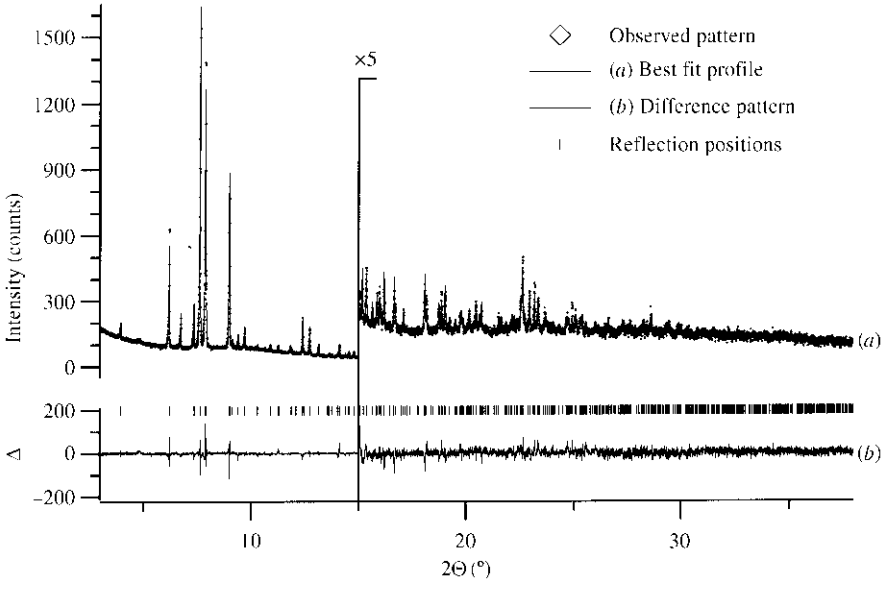


**Figure 3**
Scattered synchrotron X-ray intensity for tetraferrocenyl-[3]-cumulene at ambient conditions as a function of diffraction angle 2Θ. Shown are the observed pattern (diamonds), the best Rietveld fit profile (line), the reflection positions, and the difference curve between observed and calculated profiles as the trace at the bottom. The high-angle part is enlarged by a factor of 5 starting at 15° 2Θ. Wavelength λ = 0.70017 (2) Å. The $R$ values are $R_p = 5.1\%$, $R_{wp} = 7.5\%$, $R(F) = 16.5\%$ and $R(F^2) = 20.5\%$. $R_p$, $R_{wp}$, $R(F)$ and $R(F^2)$ refer to the Rietveld criteria of fit for profile, weighted profile and structure factor, respectively, defined in the work of Langford & Louër (1996).

single-crystal structure analysis could be collected. Twinning along the *b* axis was observed but extensive peak overlap made the determination of individual intensities almost impossible. Therefore, we relied on X-ray powder diffraction data as the only source for structural information.

The profiles of the powder peaks and precise lattice parameters were determined by fits of the Le Bail type using the program *GSAS* (Larson & Von Dreele, 1994). The background was modelled manually using *GUFI* (Dinnebier & Finger, 1998). The peak profile was described by a pseudo-Voigt function (Thompson *et al.*, 1987) in combination with a special function that accounts for the asymmetry resulting from axial divergence (Finger *et al.*, 1994).

A trace of an unidentified additional phase (<3%) was observed in several peaks in the powder pattern. No phase change was observed upon cooling from room temperature to 75 K.

## 3. Structure determination

The mismatch between the number of formula units per unit cell ($Z = 1$) and the space-group symmetry $P2_1/a$, which is not consistent with the molecular symmetry of the tetraferrocenyl-[3]-cumulene molecule, required disorder at least for the cumulene bridge. Even lowering of the space-group symmetry to $P2_1$ did not allow the construction of a unit cell consisting of fully ordered molecules. The short *b* axis of 6.1 Å indicated the possibility that the cumulene bridge is aligned along this axis.

Under the assumption that despite the anticipated disorder the average position and orientation of the tetraferrocenyl-[3]-cumulene molecules can be found in the higher symmetry space group, structure solution of tetraferrocenyl-[3]-cumulene was first tried by direct methods using the program *SIRPOW* (Cascarano *et al.*, 1992). All attempts failed, using different sets of starting parameters in both space groups $P2_1/a$ and $P2_1$. This can be understood in view of the anticipated disorder and massive accidental overlap of peaks.

Since the connectivity of the atoms was known from several single-crystal studies of related compounds (Bildstein *et al.*, 1995, 1996, 1998, 1999), structure determination for tetraferrocenyl-[3]-cumulene was carried out by means of the simulated-annealing technique (van Laarhoven & Aarts, 1987; David *et al.*, 1998) using the program *DASH* (David, 1999). The procedure uses the following information: the molecular geometry, a list of diffraction peak intensities, and a list of parameters to be varied and their ranges for the simulated-annealing runs.

For the definition of the connectivity between the atoms within the molecule, we used the *Z*-matrix notation (*e.g.* Leach, 1996), which allows the description of the entire molecule and its intramolecular degrees of freedom by using interatomic distances, angles and dihedral angles. All intramolecular angles and distances were kept fixed at standard values, allowing only the torsion angles to vary (Fig. 1).

The diffraction intensities were extracted by a Pawley-type refinement, using the program *DASH* (Pawley, 1981; David, 1999). The peak profile was modelled by the Voigt function, to which a correction for the asymmetry caused by axial divergence was applied. The background was included in the refinement process using high-order Chebyshev polynomials. The covariance matrix of the Pawley fit, which describes the degree of correlation between the individual intensities of neighbouring reflections, was used in the calculation of the level of agreement between the measured intensities and those of the trial structures after each simulated-annealing step. It was therefore not necessary to include the entire powder pattern in the simulated-annealing procedure, which considerably decreased the computing time needed for each cycle.

The Pawley fit for tetraferrocenyl-[3]-cumulene for the angular range 2–25° 2Θ (4601 data points) led to profile values of $R_p = 3.92\%$, $R_{wp} = 5.25\%$, $R_{expected} = 3.41\%$ and $\chi^2 = 2.37$.

At the beginning of the simulated-annealing runs, one ferrocene molecule and two bonded carbon atoms (C—C = 1.3 Å) with 50% occupancy, representing half of the cumulene bridge, were placed independently in the unit cell in space group $P2_1/a$. A total of 15 parameters were varied during the simulated-annealing runs [one torsion angle, $2 \times 3$ fractional parameters for the positions of the molecules, and $2 \times 4$ quaternians[1] (Leach, 1996) describing the orientation of the molecules within the unit cell]. The trial structures were generated using a set of numbers chosen randomly in a Monte Carlo fashion within the given range for the 15 parameters (Press *et al.*, 1992). The starting temperature[2] for the simulated-annealing run was set to 100 K and decreased slowly, allowing 7200 moves per temperature. The $\chi^2$ of the integrated intensities fell dramatically in the first few thousand moves, indicating that the scattering is dominated by the positioning of the Fe atom of the ferrocene molecule. Several million trial structures were generated before the minimum was reached, the process taking a few hours to run on a Digital Personal Workstation 433au. A simplex search at the end of the simulated-annealing run confirmed that a deep minimum had been obtained. Note that no special algorithms were employed to prevent close contact of molecules during the global optimization procedure. In general, these have not been found to be necessary as the fit to the structure factors alone quickly moves the molecules to regions of the unit cell where they do not grossly overlap with neighbouring molecules.

A preliminary Rietveld refinement using the program *DASH* (Rietveld, 1969; David, 1999), in which only the scale factor and the overall atomic displacement parameter were refined, provided strong evidence for the correctness of the position of the ferrocene molecule, although the fit was not entirely satisfactory. Additional simulated-annealing runs in space groups $P2_1$ and $P1$ did not show any improvement despite increasing the number of parameters.

[1] The four quaternians allow a uniform sampling over the surface of a sphere in contrast to the three Euler angles.

[2] Temperature is not a temperature in the thermodynamical sense but refers to the term $T$ in the expression $\exp(E/KT)$, which is generally known as the Boltzmann factor with the Boltzmann constant $K$ and the state of energy $E$. The analogous expression with $E = \chi^2_{new} - \chi^2_{old}$ (difference in $\chi^2$ of consecutive cycles) is used as an acceptance criterion in the simulated-annealing process.

Under the assumption that the position and the orientation of the ferrocene molecule as found by simulated annealing are approximately correct, the only possible location for the cumulene bridge is in the *ac* plane, parallel to the *b* axis, linking four ferrocene molecules of two neighbouring unit cells. The anticipated location of the cumulene bridge could then be confirmed by results from the simulated-annealing process. In this location, the carbon sites of the cumulene bridge are only half occupied, suggesting twofold disorder with an occurrence of a cumulene bridge in every second unit cell. Since the orientation of the four ferrocene molecules linked by the cumulene unit was not entirely favourable, it was quite clear that the ferrocenes must also be statistically disordered.

To avoid any biasing by the model, another simulated-annealing approach was started from scratch in space group $P2_1/a$, involving two independent ferrocene molecules with variable occupancies. The simulated-annealing process converged to a deeper minimum than before, with both ferrocene molecules having essentially the same position, the same occupancy (50%) but different orientations (Figs. 4 and 5). No further improvement could be achieved by increasing the number of disordered ferrocene molecules. At this point, we decided to switch to Rietveld refinement to elucidate the structural details further.

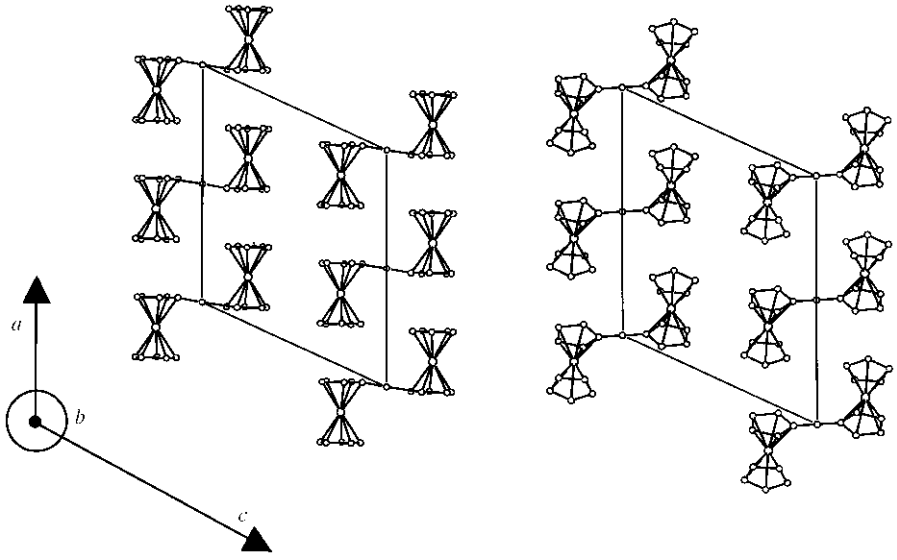


**Figure 4**
Packing diagrams of tetraferrocenyl-[3]-cumulene, perpendicular to the *b* axis, showing the two different orientations of the disordered ferrocene molecules with respect to the cumulene bridge. Hydrogen atoms are omitted for clarity.

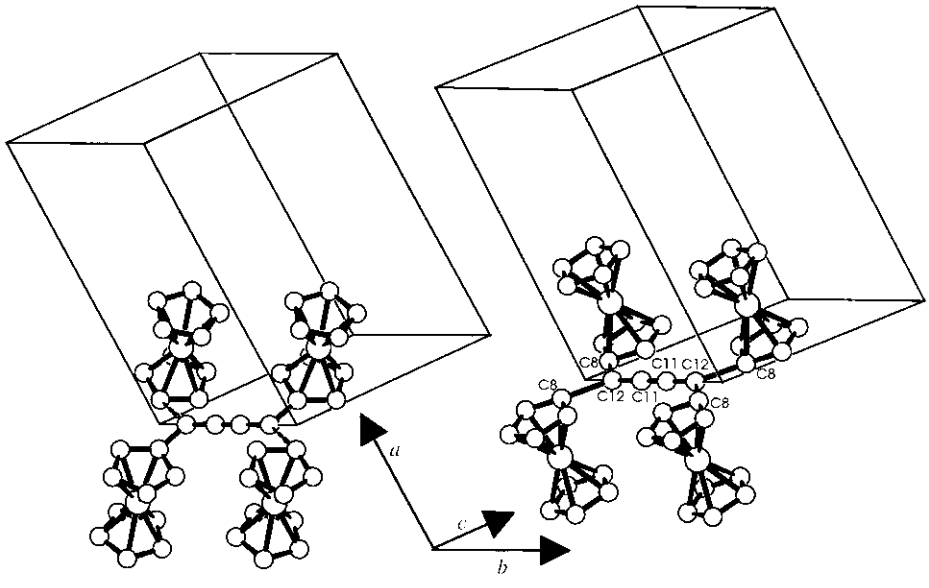


**Figure 5**
Molecular structure and unit cell of tetraferrocenyl-[3]-cumulene for the two different orientations of the disordered ferrocene molecules. Hydrogen atoms are omitted for clarity.

Rietveld refinements of the crystal structure of tetraferrocenyl-[3]-cumulene were carried out using the program *GSAS* (Larson & Von Dreele, 1994). Two rigid bodies representing the two disordered ferrocene molecules were used. This step reduced the number of refinable parameters for the ferrocenes to nine (three translations, 2 × 2 rotations and 2 × 1 torsion angle), while constraining the position of the Fe atoms to be the same. The values for the distances Fe—$\pi$($C_5H_5$) = 1.67, C—C = 1.38 and C—H = 1.05 Å were taken from the literature (Bildstein *et al.*, 1995, 1996; Bildstein, Schweiger, Kopacka, Ongania & Wurst, 1998). Any attempts to refine these lengths resulted in meaningless values because of the high correlation between the parameters.

To model the disordered cumulene bridge, two crystallographically independent carbon atoms with 50% occupancy were positioned along the *b* axis and restrained to a bond length of 1.3 Å. Their positions were fully released at the final stage of the refinement process, but did not change significantly.

The satisfactory agreement between the measured and the calculated profile for tetraferrocenyl-[3]-cumulene indicates that further refinement might not reveal more structural details. The positional parameters of the final Rietveld refinement (Fig. 3) and the

**Table 2**
Atomic coordinates, displacement parameters $U_{iso}$ (Å$^2$) and fractional occupancy of tetraferrocenyl-[3]-cumulene in $P2_1/a$ symmetry at 295 K.

The atomic displacement parameters of the $C_5H_5$ (Cp) rings and of the cumulene bridge are constrained to be equal within the molecules. The sum of the fractional occupancies of the orientations of the ferrocene molecule is constrained to be one.

| | *x* | *y* | *z* | $U_{iso}$ | Occupancy |
|---|---|---|---|---|---|
| Fe(1) | −0.19579 (22) | −0.0261 (8) | −0.25050 (25) | 0.0055 (1) | 0.505 (9) |
| C(1) | −0.35434 (100) | −0.1543 (46) | −0.3310 (27) | 0.0012 (3) | 0.505 (9) |
| C(2) | −0.35882 (75) | 0.0662 (57) | −0.3584 (18) | 0.0012 (3) | 0.505 (9) |
| C(3) | −0.30792 (138) | −0.1792 (40) | −0.1959 (31) | 0.0012 (3) | 0.505 (9) |
| C(4) | −0.31517 (154) | 0.1776 (26) | −0.2402 (37) | 0.0012 (3) | 0.505 (9) |
| C(5) | −0.28371 (91) | 0.0260 (63) | −0.1398 (12) | 0.0012 (3) | 0.505 (9) |
| H(1) | −0.3815 (19) | −0.2810 (77) | −0.40072 (490) | 0.0012 (3) | 0.505 (9) |
| H(2) | −0.3900 (14) | 0.1368 (101) | −0.45259 (295) | 0.0012 (3) | 0.505 (9) |
| H(3) | −0.2935 (25) | −0.3281 (62) | −0.14481 (575) | 0.0012 (3) | 0.505 (9) |
| H(4) | −0.3073 (28) | 0.3479 (27) | −0.22874 (670) | 0.0012 (3) | 0.505 (9) |
| H(5) | −0.2477 (14) | 0.0606 (111) | −0.03852 (171) | 0.0012 (3) | 0.505 (9) |
| C(6) | −0.05803 (122) | 0.1505 (27) | −0.2329 (29) | 0.0012 (3) | 0.505 (9) |
| C(7) | −0.10202 (93) | 0.0427 (49) | −0.3523 (15) | 0.0012 (3) | 0.505 (9) |
| C(8) | −0.02725 (32) | −0.0042 (54) | −0.1343 (10) | 0.0012 (3) | 0.505 (9) |
| C(9) | −0.09843 (121) | −0.1786 (40) | −0.3274 (23) | 0.0012 (3) | 0.505 (9) |
| C(10) | −0.05222 (121) | −0.2076 (34) | −0.1927 (27) | 0.0012 (3) | 0.505 (9) |
| H(6) | −0.0495 (23) | 0.3204 (30) | −0.21952 (530) | 0.0012 (3) | 0.505 (9) |
| H(7) | −0.1328 (15) | 0.1163 (84) | −0.44571 (241) | 0.0012 (3) | 0.505 (9) |
| H(8) | 0.0088 (7) | 0.0273 (92) | −0.03258 (129) | 0.0012 (3) | 0.505 (9) |
| H(9) | −0.1260 (21) | −0.3031 (65) | −0.39857 (409) | 0.0012 (3) | 0.505 (9) |
| H(10) | −0.0385 (22) | −0.3581 (50) | −0.14324 (488) | 0.0012 (3) | 0.505 (9) |
| Fe(1*B*) | −0.19579 (22) | −0.0261 (8) | −0.25050 (25) | 0.0055 (1) | 0.495 (9) |
| C(1*B*) | −0.35563 (100) | −0.0077 (26) | −0.2633 (32) | 0.0012 (3) | 0.495 (9) |
| C(2*B*) | −0.28927 (171) | −0.1297 (45) | −0.1545 (15) | 0.0012 (3) | 0.495 (9) |
| C(3*B*) | −0.35680 (91) | −0.1104 (41) | −0.3736 (15) | 0.0012 (3) | 0.495 (9) |
| C(4*B*) | −0.24943 (115) | −0.3077 (26) | −0.1976 (24) | 0.0012 (3) | 0.495 (9) |
| C(5*B*) | −0.29117 (165) | −0.2958 (28) | −0.3330 (23) | 0.0012 (3) | 0.495 (9) |
| H(1*B*) | −0.3978 (18) | 0.1376 (33) | −0.26234 (557) | 0.0012 (3) | 0.495 (9) |
| H(2*B*) | −0.2721 (30) | −0.0934 (77) | −0.05617 (215) | 0.0012 (3) | 0.495 (9) |
| H(3*B*) | −0.4000 (17) | −0.0569 (72) | −0.47136 (209) | 0.0012 (3) | 0.495 (9) |
| H(4*B*) | −0.1966 (16) | −0.4306 (42) | −0.13777 (430) | 0.0012 (3) | 0.495 (9) |
| H(5*B*) | −0.2757 (29) | −0.4080 (48) | −0.39437 (422) | 0.0012 (3) | 0.495 (9) |
| C(6*B*) | −0.11830 (114) | 0.2710 (13) | −0.2029 (6) | 0.0012 (3) | 0.495 (9) |
| C(7*B*) | −0.13908 (119) | 0.2183 (15) | −0.3310 (9) | 0.0012 (3) | 0.495 (9) |
| C(8*B*) | −0.04890 (73) | 0.1123 (20) | −0.1214 (10) | 0.0012 (3) | 0.495 (9) |
| C(9*B*) | −0.08252 (100) | 0.0270 (23) | −0.3286 (14) | 0.0012 (3) | 0.495 (9) |
| C(10*B*) | −0.02679 (31) | −0.0385 (26) | −0.1991 (15) | 0.0012 (3) | 0.495 (9) |
| H(6*B*) | −0.1498 (17) | 0.4079 (9) | −0.17281 (34) | 0.0012 (3) | 0.495 (9) |
| H(7*B*) | −0.1891 (17) | 0.3080 (12) | −0.41543 (68) | 0.0012 (3) | 0.495 (9) |
| H(8*B*) | −0.0183 (12) | 0.1072 (20) | −0.01835 (94) | 0.0012 (3) | 0.495 (9) |
| H(9*B*) | −0.0820 (16) | −0.0544 (27) | −0.41092 (170) | 0.0012 (3) | 0.495 (9) |
| H(10*B*) | 0.0236 (6) | −0.1785 (32) | −0.16550 (188) | 0.0012 (3) | 0.495 (9) |
| C(11) | 0.0 | 0.4092 (25) | 0.0 | 0.0016 | 0.5 |
| C(12) | 0.0 | −0.1966 (25) | 0.0 | 0.0016 | 0.5 |

overall atomic displacement parameters are presented in Table 2; a selection of geometric parameters is given in Table 3.[3]

## 4. Results and discussion

Tetraferrocenyl-[3]-cumulene forms a highly disordered structure in the solid state. Since the occupancy of the cumulene bridge is 50%, only every second cumulene bridge is formed with every ferrocene molecule still connected to one cumulene bridge. At first sight, this finding suggests a statistical disorder along the crystallographic *b* axis with polymerization of the cumulene units to dimers or higher oligomers. However, this is not possible because of the maximum of four single bonds being allowed for carbon atoms. Therefore, there cannot be disorder along the *b* axis. On the other hand, a cumulene bridge between the ferrocene molecules of every second unit cell would imply a doubling of the *b* axis.

Under the assumption of an ordered structure in the *b*-axis direction, two basic stacking sequences can be derived by shifting consecutive layers by either $+\frac{1}{4}$ or $-\frac{1}{4}$ of the doubled *b* axis in the *a* direction. Starting from a row which is assigned the position *A*, consecutive shifts by $-\frac{1}{4} \times 2b$ create rows at positions *B*, *C* and *D*, before *A* is reached again; alternate shifts of $+\frac{1}{4} \times 2b$ (or $-\frac{1}{4} \times 2b$) create one more row *B* (or *D*) (Fig. 6). The two alternative positions for the next chain give rise to an infinite number of possible packing sequences. Stacking faults then are responsible for the failure to observe the true 2*b* axis.

In a systematic approach, the possible periodic stacking sequences can be derived easily from the 'layer stacking tree' depicted in Fig. 7, which takes into account that for consecutive layers, not all combinations of *A*, *B*, *C* and *D* are allowed. It follows that there is one structure $(AB)_\infty$ [and its enantiomorph $(AD)_\infty$], with period two, and there are two structures, $(ABCD)_\infty$ and $(ABCB)_\infty$ [and their equivalents $(ADCD)_\infty$ and $(ADCB)_\infty$], with period four. Generally, only periodic structures with even periods can occur.

We will neither develop a full classification for various periodic crystal structures nor classify the various types of stacking faults, but we will show how stacking faults within two structures can lead to the observed features in the X-ray scattering. The stacking sequence of $(ABCD)_\infty$ (I) corresponds to a *C*-centred ordered supercell of $2a \times 2b \times c$ in space group *C*111 [or $(a - b) \times (a + b) \times c$ in *P*111] (Fig. 6*a*) and can be considered the counterpart of cubic close packed

[3] Structure factors, the numerical intensity of each measured point on the diffraction profile, and geometric parameters of tetraferrocenyl-[3]-cumulene at 295 K are available from the IUCr electronic archives (Reference: ZM0077). Services for accessing these data are described at the back of the journal.

**Table 3**
Selected geometric parameters (Å, °) for both orientations of the disordered crystal structure of tetraferrocenyl-[3]-cumulene.

| | |
|---|---|
| Fe–$\pi$(Cp) | 1.67 (fixed) |
| C(Cp)–C(Cp) | 1.38 (fixed) |
| C(Cp)–H(Cp) | 1.05 (fixed) |
| Fe–C(Cp) | 2.041 (fixed) |
| | |
| Fe–Fe (intramolecular) | 5.80 (2) |
| Fe–Fe (intermolecular) | 5.99 (2) |
| | |
| $FeCp_2$ deviation from staggered | 1 (2), 20 (1) |
| Angle between the two different orientations of $FeCp_2$ | 35 (2) |
| | |
| C(11)–C(11) | 1.11 (3) |
| C(11)–C(12) | 1.30 (1) |
| C(12)–C(8) | 1.34 (1)–1.86 (3) |
| | |
| H(2)–H(9) close contact (*O*1) | 1.80 (3) intermolecular |
| H(4*B*)–H(6*B*) close contact (*O*2) | 1.31 (5) intramolecular |

(c.c.p.) stacked spheres. The stacking sequence of $(AB)_\infty$ (II) corresponds to a primitive supercell of $a \times 2b \times c$ in space group $P1a1$ (Fig. 6*b*) and can be considered the counterpart of hexagonal close packed (h.c.p.) stacked spheres.

One type of stacking fault in (I) leads to fault configurations $ABCDA{:}DABCD$ (Fig. 6*a*), $ABCDAB{:}ABCD$ and $ABCDABC{:}BCD$,[4] which can be viewed as the insertion of type (II) stacking sequences *DA*, *BC* or *AB*. Another type of stacking fault in (II) leads to a fault configuration $ABA{:}DAD$ (Fig. 6*b*), which adopts locally the stacking from type (I) sequences.

Stacking disorder in true h.c.p. and c.c.p. stackings of spheres always leads to *area* defects, whereas in our case, stacking disorder within a layer of chains of ordered molecules leads to *line* defects. A low stacking-fault energy for these line defects can be expected, which enhances the occurrence of stacking faults in the crystal structure of tetraferrocenyl-[3]-

[4] Dotted lines represent the location of the fault line with respect to the initial stacking sequence on the left-hand side.

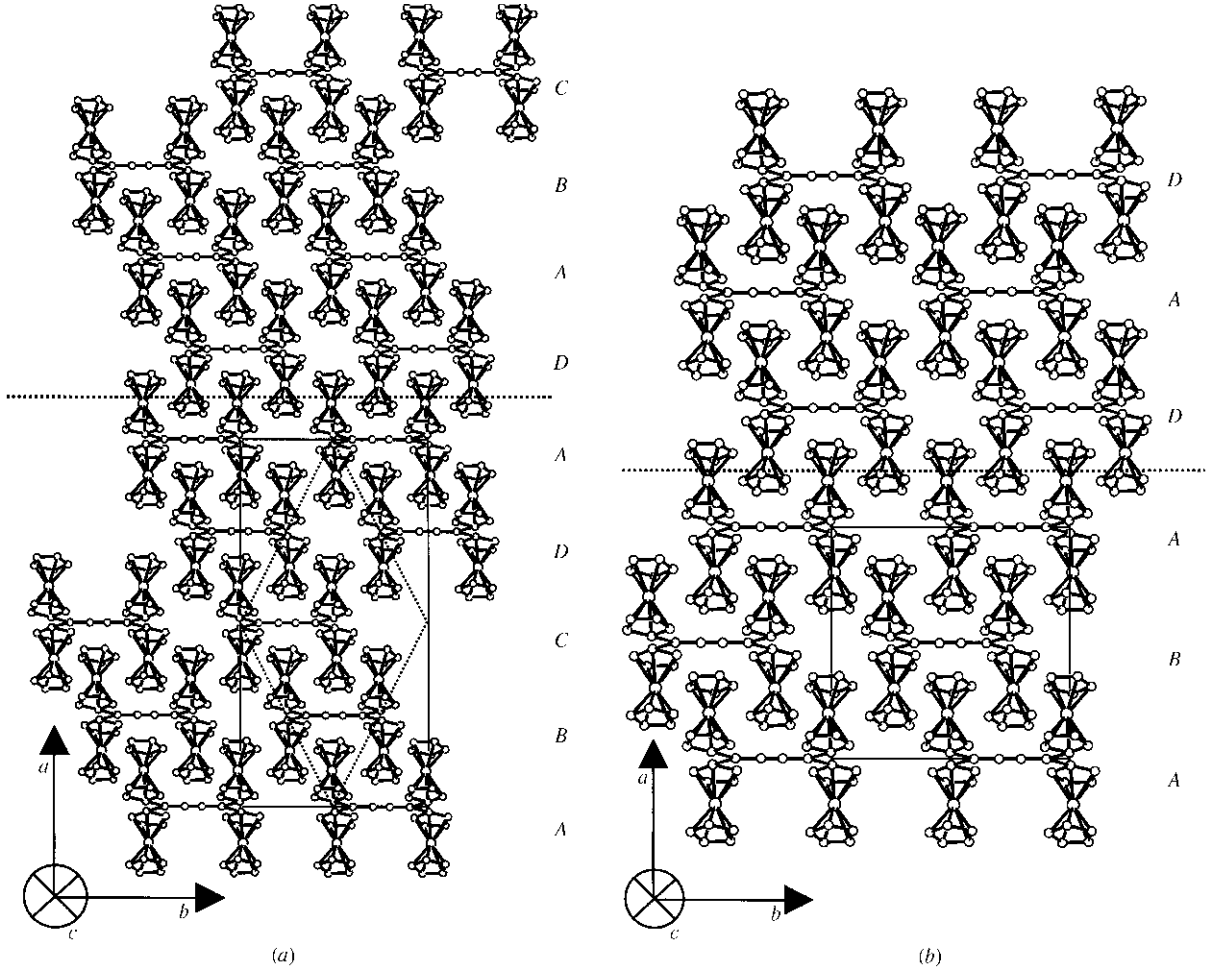


**Figure 6**
Packing diagrams of tetraferrocenyl-[3]-cumulene, perpendicular to the *c* axis. Only one orientation of the disordered ferrocene molecules is drawn. Two possible stackings leading to different supercells are shown: (*a*) $(ABCD)_\infty$ structure with $a' = 2a$, $b' = 2b$, $c' = c$ and space group $C111$; (*b*) $(AB)_\infty$ structure with $a' = a$, $b' = 2b$, $c' = c$ and space group $P1a1$. For (*a*), the primitive cell $a' = a - b$, $b' = a + b$, $c' = c$ in $P111$ is also shown. The dashed horizontal lines symbolize the stacking faults. Hydrogen atoms are omitted for clarity. The nomenclature for the different layers is given on the right-hand side.

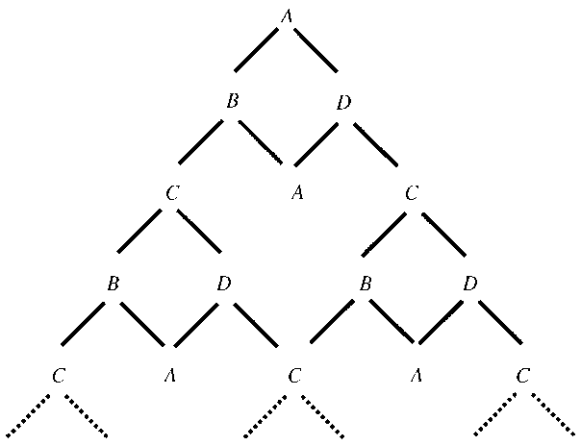


**Figure 7**
Tree-like representation of all allowed combinations of layers up to the fourth period for tetraferrocenyl-[3]-cumulene starting from layer *A*.

cumulene. A high stacking-fault density with a statistical occurrence of stacking faults after short periods of ordered stacking is necessary to explain the small unit cell as found by X-ray diffraction.

The stacking faults of the chains (line defects) in different layers perpendicular to the *c* axis are independent of one another. It is therefore likely that additional stacking faults occur between layers stacked perpendicular to the *c*-axis direction (area defects) and they will further enhance the disorder. In the case of two independent types of disorder in the *a* and *c* directions, we would *not* expect anisotropic broadening of the reflections, which is in agreement with the observed powder pattern.

It should be noted that although stacking faults are frequently observed in metals, alloys, spherically shaped materials, like $C_{60}$, and inorganic materials, they rarely occur in coordination compounds, which makes the structure of the title compound an exceptional example.

In the small unit cell as found by X-ray diffraction, all four ferrocene molecules of one tetraferrocenyl-[3]-cumulene molecule are created by space-group symmetry out of one staggered ferrocene molecule in general position. The normals of the cyclopentadienyl rings are oriented parallel to the crystallographic *a* axis. Some of these ferrocene molecules are in a slightly unfavourable orientation (*O*1) towards the cumulene bridge, indicating that (at least) one other orientation exists. Simulated annealing and rigid-body Rietveld refinement confirmed a second orientation (*O*2) of the ferrocene molecule in the asymmetric unit, with 50% occupancy and rotated by approximately 35° around the *c** direction with respect to the first orientation (*O*1). The second orientation describes a ferrocene molecule in a conformation that is about 20° away from staggered. No evidence for a superstructure or for lower space-group symmetry was found.

In accordance with the results from X-ray diffraction, there are eight possible molecular conformations (or combinations of them) to combine the two different orientations (*O*1 and *O*2) equally over space:

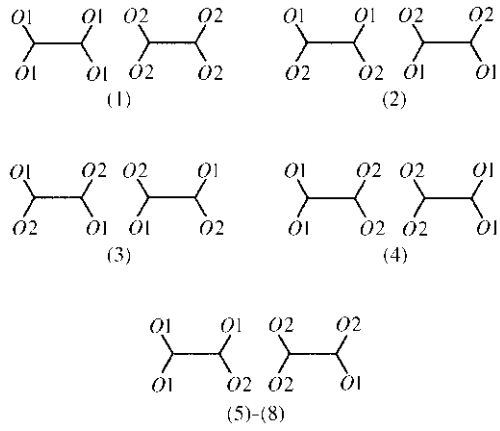


The bond lengths between the cumulene bridge and the ferrocene molecules are either too long or too short (Table 3), which can be attributed to the disorder in combination with the low information content of the powder pattern. Nevertheless, for two cross-linked orientations *O*1 and two cross-linked orientations *O*2, the bond lengths are closer to the expected values. This finding increases the probability for combination (3).

In contrast to all other compounds of this class (Bildstein *et al.*, 1995, 1996; Bildstein, Schweiger, Kopacka, Ongania & Wurst, 1998), the ferrocenyl groups are in a *syn* rather than in an up–down conformation with respect to the cumulene bridge. However, in solution, all four ferrocenyl substituents are magnetically equivalent (by NMR) (Bildstein, Schweiger, Kopacka & Wurst, 1998); therefore, the unusual *syn* conformation in the solid state has to be attributed to crystal packing effects.

## 5. Conclusions

It has been shown that a moderately complex crystal structure of a coordination compound can nowadays be solved from high-resolution powder data even in the presence of severe disorder, using the powerful combination of simulated annealing and rigid-body Rietveld refinement. It is therefore possible to derive plausible models for stacking faults and orientational disorder of molecules even from powder data. The computer time for solution of the basic structure is typically of the order of several hours. On the other hand, one has to be aware of the limitations of the powder method arising from systematic and accidental peak overlap in the powder pattern. The latter is severe in the present case. It was indisputably possible to determine the molecular conformations with fairly high precision, but it was not possible to determine individual bond lengths and angles within the disordered molecules.

Research was carried out in part at the National Synchrotron Light Source at Brookhaven National Laboratory, which is supported by the US Department of Energy, Division of Materials Sciences and Division of Chemical Sciences. The

SUNY X3 beamline at NSLS is supported by the Division of Basic Energy Sciences of the US Department of Energy under Grant No. DE-FG02-86ER45231. This research was funded by the Deutsche Forschungsgemeinschaft (Di 687-2) and by the FWF (P13073-PHY), Vienna, Austria.

## References

Andreev, Y. G. & Bruce, P. G. (1998). *Mater. Sci. Forum*, **278–281**, 14–19.
Andreev, Y. G., Lightfoot, P. & Bruce, P. G. A. (1997). *J. Appl. Cryst.* **30**, 294–305.
Andreev, Y. G., MacGlashan, G. S. & Bruce, P. G. (1997). *Phys. Rev. B*, **55**, 12011–12017.
Bendele, G. M., Stephens, P., Prassides, K., Vavekis, K., Kordatos, K. & Tanigaki, K. (1998). *Phys. Rev. Lett.* **80**, 736–739.
Bildstein, B., Denifl, P., Wurst, K., André, M., Baumgarten, M., Friedrich, J. & Ellmerer-Müller, E. (1995). *Organometallics*, **14**, 4334–4342.
Bildstein, B., Kopacka, H., Schweiger, M., Ellmerer-Müller, E., Ongania, K.-H. & Wurst, K. (1996). *Organometallics*, **15**, 4398–4406.
Bildstein, B., Schweiger, M., Angleitner, H., Kopacka, H., Wurst, K., Ongania, K.-H., Fontani, M. & Zanello, P. (1999). *Organometallics*, **18**, 4286–4295.
Bildstein, B., Schweiger, M., Kopacka, H., Ongania, K.-H. & Wurst, K. (1998). *Organometallics*, **17**, 2414–2424.
Bildstein, B., Schweiger, M., Kopacka, H. & Wurst, K. J. (1998). *J. Organomet. Chem.* **553**, 73–81.
Bruce, M. I. (1998). *Chem. Rev.* **98**, 2797–2858.
Bruce, M. I. (1997). *Coord. Chem. Rev.* **166**, 91–119.
Cascarano, G., Favia, L. & Giacovazzo, C. (1992). *J. Appl. Cryst.* **25**, 310–317.
Chernyshev, V. V. & Schenk, H. (1998). *Z. Kristallogr.* **213**, 1–3.
Cox, P. E. (1991). *Handbook on Synchrotron Radiation*, Vol. 3, edited by G. Brown & De. E. Moncton, ch. 5. Amsterdam: Elsevier.
David, W. I. F. (1999). *DASH. Simulated-Annealing Program.* Personal communication.
David, W. I. F., Shankland, K. & Shankland, N. (1998). *Chem. Commun.* pp. 931–932.
Dinnebier, R. E., Olbrich, F., Schneider, M., van Smaalen, S. & Behrens, U. (1999). *Acta Cryst.* B**55**, 35–44.
Dinnebier, R. E., Stephens, P. W., Carter, J. K., Lommen, A. N., Heiney, P. A., McGhie, A. R., Brard, L. & Smith, A. B. III (1995). *J. Appl. Cryst.* **28**, 327–334.
Dinnebier, R. E. & Finger, L. (1998). *Z. Kristallogr. Suppl.* **15**, 148.
Finger, L. W., Cox, D. E. & Jephcoat, A. P. (1994). *J. Appl. Cryst.* **27**, 892–900.
Fischer, H. (1964). *Cumulenes*, in *The Chemistry of Alkenes*, edited by S. Patai, ch. 13, p. 1025. London: Interscience/John Wiley.
Hopf, H. (1980). *The Preparation of Allenes and Cumulenes*, in *The Chemistry of Ketenes, Allenes and Related Compounds*, edited by S. Patai, part 2, ch. 20, p. 781. Chichester: Interscience/John Wiley.
Kariuki, B. M., Calcagno, P., Harris, K. D. M., Philip, D. & Johnston, R. L. (1999). *Angew. Chem. Int. Ed. Engl.* **38**, 831–835.
Langford, J. I. & Louër, D. (1996). *Rep. Prog. Phys.* **59**, 131–234.
Larson, A. C. & Von Dreele, R. B. (1994). *GSAS – General Structure Analysis System*, Los Alamos National Laboratory Report LAUR 86-748, available *via* anonymous FTP from mist.lansce.lanl.gov.
Leach, A. R. (1996). *Molecular Modelling Principles and Applications*, pp. 2–4. London: Addison Wesley Longman.
Le Bail, A. (1999). *Structure Determination from Powder Diffraction – Database*, http://fluo.univ-lemans.Fr:8001/iniref.html.
MacGlashan, G. S., Andreev, Y. G. & Bruce, P. G. (1999). *Nature (London)*, **398**, 792–794.
Masciocchi, N., Moret, M., Cairati, P., Ragaini, F. & Sironi, A. (1993). *J. Chem. Soc. Dalton Trans.* pp. 473–475.
Newsam, J. M., Deem, M. W. & Freeman, C. M. (1992). *Accuracy in Powder Diffraction II*, *NIST Spec. Publ.* No. 846, pp. 80–91.
Paul, F. & Lapinte, C. (1998). *Coord. Chem. Rev.* **178–180**, 431–509.
Pawley, G. S. (1981). *J. Appl. Cryst.* **14**, 357.
Press, W. H., Teukolsky, S. A., Vetterling, W. T. & Flannery, B. P. (1992). *Numerical Recipes in Fortran 77*, 2nd ed. Cambridge University Press.
Rietveld, H. M. (1969). *J. Appl. Cryst.* **2**, 65–71.
Rius, J., Miravittles, C., Gies, H. & Amigo, J. M. (1999). *J. Appl. Cryst.* **32**, 89–97.
Schmidt, M. U. & Dinnebier, R. E. (1999). *J. Appl. Cryst.* **32**, 178–186.
Shankland, K., David, W. I. F. & Csoka, T. (1997). *Z. Kristallogr.* **212**, 550–552.
Thompson, P., Cox, D. E. & Hastings, J. B. (1987). *J. Appl. Cryst.* **20**, 79–83.
Touchard, D. & Dixneuf, P. H. (1998). *Coord. Chem. Rev.* **178–180**, 409–429.
Tremayne, M., Kariuki, B. M. & Harris, K. D. M. (1996). *Mater. Sci. Forum*, **278–281**, 32–37.
Tremayne, M., Kariuki, B. M., Harris, K. D. M., Shankland, K. & Knight, K. S. (1997). *J. Appl. Cryst.* **30**, 968–974.
Van Laarhoven, P. J. M. & Aarts, E. H. L. (1987). *Simulated Annealing: Theory and Applications*. Dordrecht: D. Reidel.
Visser, J. W. (1969). *J. Appl. Cryst.* **2**, 89–95.
Von Dreele, R. B. (1999). *J. Appl. Cryst.* **32**, 1084–1089.